

Formation and Growth of Nuclei and the Growth of Interfaces in the Chemical Decomposition of Solids: New Insights[†]

P. W. M. Jacobs

Department of Chemistry, The University of Western Ontario, London, Ontario, Canada N6A 5B7

Received: May 8, 1997; In Final Form: July 10, 1997[®]

Solid-state reactions generally start at specific sites, the first-formed product at these sites being referred to as “the nuclei”. From a general law of nucleus formation, the simpler equations commonly encountered follow. Further reaction takes place at the interface between nuclei and reactant so that the first-formed nuclei grow in size. Visual observation of large nuclei shows that these grow at a constant rate, but in many solid-state decompositions, experimental evidence suggests a slower rate of growth for small nuclei, because the general kinetic equation based on nucleus formation and a constant rate of growth fails to adequately describe the early stages of the reaction before the rapid acceleratory process. The questions of long induction periods and the slower growth of nuclei at first are addressed, and a general phenomenological model is developed. This is applied to three different examples, and its applicability in three such varied cases suggests that it might prove to be of much wider use in reactions with long induction periods. In some reactions, structural changes induced by the reaction result in the multiplication (“branching”) of nuclei and a general equation (of which the Prout–Tompkins equation is a special case) is derived. This general equation is shown to fit experimental data over a wider range than the original Prout–Tompkins equation.

1. Nucleus Formation

The advancement of a reaction $A(s) = B(s) + C(g)$ may be followed by measurement (or calculation) of $a(t)$, which is defined as the fraction of A transformed in time t ,

$$a(t) = \frac{A(0) - A(t)}{A(0) - A(\infty)} \quad (1.1)$$

If the reaction is complete, then $A(\infty)$ is zero. It is an empirical fact that the chemical reaction involving a solid starts at specialized centers called nucleus-forming sites.¹ It does this because such centers are regions where chemical reaction is facilitated by some crystal imperfection, commonly a point, line, or planar defect or a chemical impurity. The first-formed product at these sites is referred to collectively as “nuclei”, and these nuclei grow in time, leading (usually) to the ultimate consumption of the reaction, $a = 1$. The first atom of the product formed may be a stable nucleus capable of immediate growth, or it may be unstable until reaching a certain critical size. The instability of small nuclei may be due to the importance of their surface Gibbs energy, as has been emphasized in connection with phase transitions,² or it may be because of the reversibility of the chemical process. Even if the initial decomposition act is irreversible, the first-formed product may not become a stable growth nucleus until it reaches a critical size if the special conditions that promote nucleus growth require more than one atom of product to develop.³ Thus, the formation of a stable growth nucleus in general requires p product atoms where $p \geq 1$. If $p > 1$, then nuclei containing i product atoms where $i < p$ are called germ nuclei. Once a growth nucleus is formed, it may grow initially at a slower rate, but ultimately, nuclei grow at a constant rate, as has been verified experimentally from the direct measurement of nuclei of visible sizes.^{4–8}

The general problem of multistep nucleation with the possibility of different rate constants for successive steps was solved

by Allnatt and Jacobs.³ The general solution³ for $n_i(t)$, where n_i is the number of nuclei containing i atoms of product, is a complicated expression but is somewhat simplified by the assumption that the rate constants k_i for the addition of the next atom to a nucleus containing i atoms are all unequal, leading to

$$n_i(t) = k_{i-1}k_{i-2}\dots k_1k_0n_0(0)\sum_{l=0}^{l=i}\exp(-k_l t)\left\{\prod_{\substack{j=0 \\ j \neq l}}^i(k_j - k_l)\right\}^{-1} \quad (1.2)$$

$n_0(0)$, being $n_i(t)$ with $i = 0$ at $t = 0$, is the number of potential nucleus-forming sites. For $k_j t \ll 1$, for all j ,

$$n_i(t) = k_{i-1}k_{i-2}\dots k_1k_0n_0(0)/i!t^i = n_0k_{in}t^i \quad (1.3)$$

where $n_0 = n_0(0)$, suggesting a general power law for nucleation at small t . In the more general case of k_j , all different for $j = 0, 1, 2, \dots, r$ but $k_j = k$ for $j > r$, the general solution again reduces to a power law,

$$n_i(t) = k^{i-r-1}k_rk_{r-1}\dots k_0n_0(0)/(i-r-1)!(r+1)!t^i = n_0k_{in}t^i \quad (1.4)$$

provided $k_j t \ll 1$. The reason why these limiting cases are important in practice is that nucleation is often unimportant for long reaction times since the reaction is proceeding principally by the growth of already-formed nuclei. Equations 1.3 and 1.4 are generalizations of Bagdassarian's earlier consideration⁹ of multistep nucleation, which, however, suffered from the restrictive assumption that $k_j = k_0$, $0 < j < p$. In this case,

$$n_i(t) = n_0(0)\{(k_0 t)^i/i!\}\exp(-k_0 t) \quad (1.5)$$

which reduces to the power law

$$n_i(t) = n_0(0)(k_0 t)^i/i! = n_0k_{in}t^i \quad (1.6)$$

and which is clearly also the limiting case of (1.3) with $k_j = k_0$.

[†] Dedicated to Sir John Meurig Thomas on the occasion of his 65th birthday.

[®] Abstract published in *Advance ACS Abstracts*, October 15, 1997.

[However, the general case may not be obtained from (1.2) but must be rederived from the set of coupled differential equations that describe the addition of successive atoms of product to a nucleus.^{3,10}] The assumption that k_j are all equal is not very appealing chemically, since the nucleus-forming site (for example, a crystal imperfection) is inevitably altered by the presence of successive product atoms. However, in the power law limit of short times, it does not matter from a kinetic point of view, although the interpretation of k_{in} , and its energy of activation, would be affected.

If indeed $p = 1$, then random (irreversible) nucleation at n_0 nucleus-forming sites implies

$$dn_1/dt = k_0(n_0 - n_1) \quad (1.7)$$

which, with boundary condition $n_i = 0$ at $t = 0$, gives

$$n_1 = n_0[1 - \exp(-k_0t)] \quad (1.8)$$

If the characteristic time for nucleation $t_n (=1/k_0)$ is much shorter than the observation times, then nuclei are formed essentially instantaneously and

$$n_1 = n_0 \quad (k_0t \gg 1) \quad (1.9)$$

But if $k_0t \ll 1$,

$$n_1 = k_0n_0t \quad (\text{linear law}) \quad (1.10)$$

as has been observed experimentally in some dehydration reactions.^{4,6} If $p = 2$ and $k_0t \ll 1$,

$$n_2 = k_2t^2 \quad (1.11)$$

and the number of nuclei would increase as the square of the time, as found for the dehydration of nickel sulfate heptahydrate.⁵ In the thermal decomposition of barium azide, the number of nuclei increase as the cube of the time.⁷ One anticipates that decomposition would start with the reaction of two electronically excited azide ions to yield $3N_2$, implying a t^2 law; alternative interpretations of the t^3 law for BaN_6 have been proposed.¹¹ The model for nucleation described above presupposes that the addition of an atom of product occurs through thermal activation and consequent reaction of atoms adjacent to the nucleus-forming site or, alternatively, if homogeneous production of an active intermediate is involved, diffusion of this intermediate through A is not rate-determining. When nucleation involves the diffusion of an intermediate product (say A^*), either the transport of A^* or the reaction of A^* at the nucleus site might be rate-determining, and in general, one can define the rate constant for the addition of the $(i + 1)$ th atom to the nucleus by²

$$k_i = k_R k_D / (k_R + k_D) \quad (1.12)$$

where k_R is the rate constant when the reaction at the interface is rate-controlling and $k_D = 4\pi D r_z$ is the rate constant for diffusion control, with D being the diffusion coefficient for the diffusing species and r_z the radius of the reaction zone which might be greater than the radius of the reaction site, particularly for the combination of oppositely charged species. For example, in the recombination of an interstitial with a cation vacancy in AgCl, molecular dynamics calculations¹² have shown that recombination occurs (by vacancy jumps) as soon as the interstitial is in the second neighbor cell. Here the directed vacancy jumps occur because of the Coulomb interaction between interstitial and vacancy. Of course, this particular

computer experiment refers to the recombination of defects² rather than to nucleus formation, but the same principles are involved.

2. Nucleus Growth

It is a matter of experimental observation that many solid-state reactions start at specialized crystal sites, the nucleus-forming sites, and that thereafter reaction proceeds preferentially at the interface between the nucleus of solid product C and the reactant A. Ideally, one might think of this as a more-or-less coherent interface between the two solids C and A, but this is not always the case; for example, it might consist of a molten zone.¹³ In the event of instantaneous nucleation on the surface of the reactant, the reaction spreads over the surface by the growth of these nuclei. If surface growth is much faster than the rate of penetration into the crystal, then a coherent interface is formed between the decomposed outer layers and reactant. If the propagating interface penetrates into undecomposed reactant at a constant rate, then the kinetics are controlled by

$$1 - (1 - a)^{1/n} = kt \quad (2.1)$$

with $n = 3$, which is sometimes termed the contracting-volume equation. For reactions spreading in two dimensions (over a surface), $n = 2$. Equation 2.1 often provides an excellent fit to the decay period of a decomposition and is particularly effective when surface nucleation and surface growth occur rapidly and internal nucleation either does not occur or occurs only very slowly. Various modifications of (2.1) are possible by retaining the concept of inward growth of surface nuclei and combining it with random nucleation and/or a finite rate of surface growth.¹⁴⁻¹⁷

The development of general kinetic equations for the decomposition of A(s) is only feasible provided nucleation is random as is the growth rate constant (though see also section 4). Certain, perhaps many, of the potential nucleus-forming sites may never become active growth nuclei because they become consumed by the growth of other nuclei. Similarly, growing nuclei must eventually impinge on one another. This ingestion of phantom nuclei by growing nuclei and the overlap of growing nuclei can be allowed for in a general way by using the concept of the extended fractional decomposition, a_{ex} , namely the fractional decomposition in time t had ingestion and overlap not occurred. a_{ex} may, of course, exceed one. Because both nucleation and growth involve decomposition events that are random in space and time, in the sense that topochemically equivalent elements of reactant all have the same probability of decomposition, in a given time increment dt

$$da = da_{ex}(1 - a) \quad (2.2)$$

which satisfies the necessary boundary conditions $da/dt = da_{ex}/dt$ at $a = 0$ and $da/dt = 0$, but da_{ex}/dt is finite, at $a = 1$. With initial conditions $a = 0$, and $a_{ex} = 0$ at $t = 0$,

$$-[\ln(1 - a)] = a_{ex} \quad (2.3)$$

The extended fractional decomposition is

$$a_{ex} = \frac{V(t)}{V(\infty)} = \frac{\sigma}{V(\infty)} \int_0^t \int_a^t g_1(x') dx' \int_a^t g_2(y') dy' \int_a^t g_3(z') dz' \left[\frac{dn}{dt} \right]_{t=0} du \quad (2.4)$$

where $V(t)$ is the volume of all growth nuclei at time t , σ is a

shape factor (e.g., $= 4\pi/3$ for spherical nuclei), $g_1(x')$ is the growth rate in the x direction at time $t = x'$, and dn/dt is the rate of formation of growth nuclei. A simple analytical solution is practicable for constant growth rates, $g_1(t) = g_1$, and, similarly, for then

$$a_{\text{ex}} = \frac{\sigma}{V(\infty)} \int_0^t g_1 g_2 g_3 (t-u)^3 \left[\frac{dn}{dt} \right]_{t=u} du \quad (2.5)$$

For multistep nucleation with $k_1 t \ll 1$,

$$n_p(t) = n_0 k_{pn} t^p \quad (2.6)$$

where p is the number of atoms of product in a nucleus for it to become a growth nucleus, and

$$\alpha_{\text{ex}} = \frac{\sigma}{V(\infty)} \int_0^t g_1 g_2 g_3 (t-u)^3 p k_{pn} n_0 u^{p-1} du \quad (2.7)$$

$$\alpha_{\text{ex}} = \frac{6\sigma g_1 g_2 g_3 n_0 k_{pn} t^{p+3}}{(p+1)(p+2)(p+3)V(\infty)} \quad (2.8)$$

$$-[\ln(1-a)] = (kt)^n \quad (2.9)$$

which is the Erofe'ev equation,¹⁸ with k being the rate constant, given by

$$k^n = (6\sigma g_1 g_2 g_3 n_0 k_{pn}) / (p+1)(p+2)(p+3)V_{\infty} \quad (2.10)$$

and exponent $n = p + 3$. For small values of a , the fractional decomposition may be approximated by a_{ex} so that the early stages of the acceleratory period ought to be described by a power law. If growth in one particular direction is very fast, then this growth rate does not control the kinetics; in this circumstance, the fractional decomposition is still given by (2.9), but with $n = p + 2$ and g_3 replaced by d_3 , the total length of the filaments of product that are formed very rapidly. For example, one can envisage decomposition starting at the points of emergence of dislocations in the surface, spreading rapidly down the dislocation cores, and thereafter segments of nuclei resembling, expanding cylinders. Similarly, growth might be rapid in two dimensions, e.g., in a grain boundary, and thereafter controlled by growth of the interface in one dimension. Thus, (2.8) may hold with a linear nucleation law, $p = 1$ ($k_{1n} = k_0$), or for instantaneous nucleation with $p = 0$, $k_{0n} = 1$. So there may be ambiguities about the interpretation of $n = p + \lambda$, where λ is the number of dimensions in which growth is rate-determining. With $p = 0, \dots, 3$ and $\lambda = 1, \dots, 3$, n may be any integer between 1 and 6. The remarkable fact is that the kinetics of the thermal decomposition of a large number of solids are described by the Erofe'ev equation (eq 2.9). Wischin⁷ found noninteger values of $n > 6$ for the decomposition of BaN_6 , and the reason for this has been discussed by Tompkins¹¹ (see also section 4).

If $p = 1$ but $k_0 t$ is not $\ll 1$, with constant growth rates in three dimensions,

$$a_{\text{ex}} = (\sigma/V(\infty)) \int_0^t g_1 g_2 g_3 (t-u)^3 k_0 n_0 \exp(-k_0 u) du \quad (2.11)$$

$$-[\ln(1-a)] =$$

$$\frac{6\sigma g_1 g_2 g_3 n_0}{V(\infty)k_0^3} \left\{ \exp(-k_0 t) - 1 + k_0 t - \frac{(k_0 t)^2}{2!} + \frac{(k_0 t)^3}{3!} \right\} \quad (2.12)$$

which is called the Avrami equation.^{19,20} The graphical representation of (2.12) in Figure 1a shows the sigmoid shape

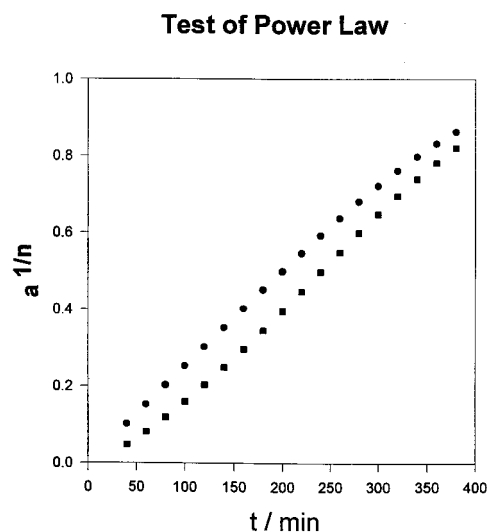
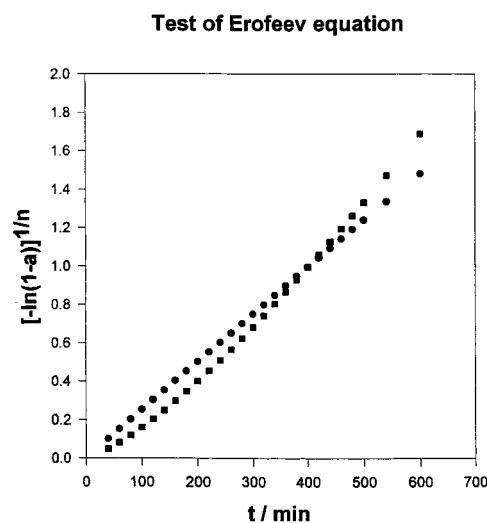
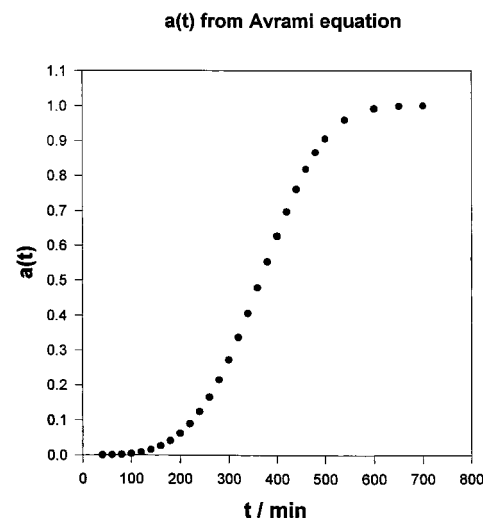


Figure 1. (a, top) Graphical representation of data that obey the Avrami equation (eq 12). (b, middle) Plots of $[-\ln(1-a)]^{1/n}$ against t for data calculated from the Avrami equation (eq 12); circles, $n = 4$; squares, $n = 3$. (c, bottom) Test of the power law using the same data as in a. Circles, $n = 4$; squares, $n = 3$.

so characteristic of many solid-state decomposition reactions. In the early part of the acceleratory period, $a \ll 1$, and for $k_0 t \ll 1$,

$$-[\ln(1-a)] \approx (kt)^4 \quad (2.13)$$

a result already contained in (2.9) since $p = 1$ and $\lambda = 3$. But if $k_0 t \gg 1$,

$$-[\ln(1 - a)] \approx (kt)^3 \quad (2.14)$$

which is the Erofe'ev equation for three-dimensional growth of a fixed number of nuclei. If $p > 1$ and $k_0 t$ is not $\ll 1$, an analytical solution is still possible,³ with $-\ln(1 - a)$ becoming a sum of terms like the right side of (2.12), though it is doubtful if this result (the generalized Avrami equation) would be of much practical use in a kinetic analysis. Traditionally, n in (2.9) has been determined graphically by plotting $[-\ln(1 - a)]^{1/n}$ vs t for various integer values of n . Figure 1b shows plots of $[-\ln(1 - a)]^{1/n}$ vs t for "data" calculated from the Avrami equation. One can see that the data are quite well fitted by straight lines with both $n = 4$ and 3 over substantial ranges of a . A more satisfactory procedure for testing for Avrami kinetics is therefore the computer fitting of experimental data for a directly to various model equations.²¹

The line for $n = 4$ in Figure 1b fits the data for $0 < a < 0.76$ and that for $n = 3$ for $0.63 < a < 1$ (see (2.13) and (2.14)). When the Erofe'ev equation (or any other suitable expression) is shown to fit experimental data for $t > t_0$,

$$[-\ln(1 - a)]^{1/n} = k(t - t_0) \quad (2.15)$$

t_0 is referred to as the induction period. For small a , $-\ln(1 - a) \approx a$, so (2.15) reduces to the power law $a^{1/n} = k(t - t_0)$. Figure 1c shows two plots of the data generated from the Avrami equation in the form of the power law with $n = 4$ and 3. The curve for $n = 4$ is linear up to $t = 240$ min, which corresponds to $a = 0.13$. The curve for $n = 3$ is a low-amplitude oscillation about a straight line, emphasizing the need for data of the highest quality possible and for great care in interpreting graphical representations of the kinetic equations.

Experimental observations of the linear rate of growth of small nuclei are limited to nuclei that are large enough to be visible, and these already contain many thousands of atoms. There is, therefore, a gap in our knowledge about the rate of growth of small nuclei. It is not altogether surprising that the rate of decomposition at very small nuclei appears in many reactions to be lower than that at large nuclei where there is a macroscopic, or at least mesoscopic, interface between product and reactant. The experimental evidence for this is the failure of an appropriate kinetic equation, for example, the Avrami equation represented in Figure 1a, to fit experimental data down to $t = 0$ and $a = 0$. An induction period to the main decomposition has traditionally been explained^{11,14} by the hypothesis of the slow growth of small nuclei. In some reactions, it is possible to separate off some preliminary process (surface decomposition) occurring before the slow growth of nuclei within the bulk of the reactant. The various stages that might be recognized during the thermal decomposition of a solid, $A(s) = B(s) + C(g)$, are shown in Figure 2, although not all of these can necessarily be distinguished in every reaction. Ammonium perchlorate²¹ is a special case for although chemical decomposition yields only gaseous products, it does not decompose completely at low temperatures and the approximately 30% residue of NH_4ClO_4 forms porous coral-like structures^{22,23} which form the growing nuclei. In Figure 2, I is a rapid deceleratory process involving nucleus formation at special (defect) sites in the surface. The extent of reaction a_s is very small because the special conditions that made these sites unstable are removed by reaction and not perpetuated. II is the induction period during which nuclei are formed at less favorable sites. It includes some initial growth of these nuclei

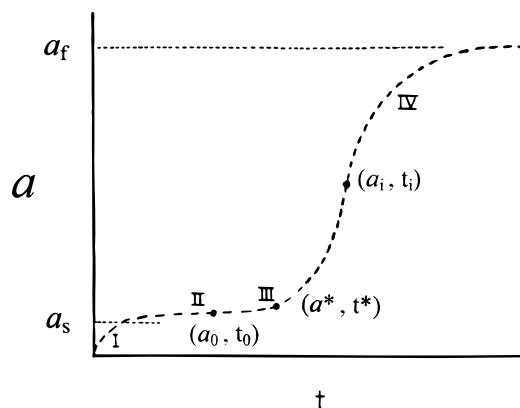


Figure 2. General form of the $a(t)$ decomposition curve that results from nucleus formation and growth. a_s represents the extent of the initial process (I) and a_0, t_0 marks the end of the induction period (II). The slow growth of nuclei (III) is followed at a^*, t^* by a rapidly accelerating reaction due to a constant rate of nucleus growth. The main part (IV) of the $a(t)$ curve is generally sigmoid in shape, the final deceleratory period ($a > a_i$) being due to consumption of reactant.

and terminates at a_0, t_0 . III represents a recognizable period of slow growth kinetics, followed at a^*, t^* by a rapid acceleration of the reaction as the nuclei grow at a constant rate. Commonly, Avrami or Erofe'ev kinetics can be expected to hold. The shape of the $a(t)$ curve during the main part of reaction IV is generally sigmoid in character, with a point of inflection at a_i, t_i , after which the rate is deceleratory because of the consumption of reactant. The Avrami–Erofe'ev models include the effect of a finite mass of reactant (through (2.3)); alternatively, if the acceleratory period is absent or of very limited duration, a predominately decay period may often be fitted by the contracting-volume equation (eq 2.1 with $n = 3$) or the unimolecular decay law which simply states that the probability of decomposition of a molecule of $A(s)$ is proportional to the amount of reactant, $da/dt = k_d(1 - a)$, so that

$$-[\ln(1 - a)] = k_d t \quad (2.16)$$

which is just the limiting case of (2.9) with $p = 0$ and $\lambda = 1$.

If compact nuclei are not observed or their existence is not inferred from Avrami–Erofe'ev kinetics, an acceleratory reaction could be taken to indicate that the nucleation process generates other nuclei so that the rate of nucleation is no longer proportional to $n_0 - n$ but instead soon (for $a > a_0 = a(t_0)$) becomes proportional to the amount of material decomposed so that

$$da/dt = k_b a \quad a \geq a_0 \quad (2.17)$$

$$a = a_0 \exp\{k_b(t - t_0)\} \quad (2.18)$$

and the fraction decomposed increases exponentially with time.^{24,25} A possible physical model is that reaction starts on the surface and spreads through the grain boundary network, the propagating nuclei branching at each node. But this process would leave isolated blocks of material covered with product and which must then decompose by inward penetration of the interface, a process which is likely to obey the unimolecular decay law (eq 2.16). Alternatively, reaction might continue by the formation and growth of internal nuclei. Thus, an exponential law during the induction period might be taken to indicate branching chains of nuclei, though another interpretation is possible (see section 4). Direct observation of nuclei is, as always, highly desirable if practicable. However, if the kinetics

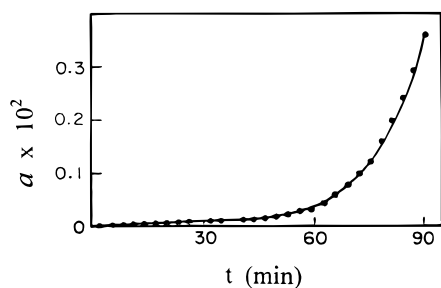


Figure 3. Least-squares fit over the induction period of data from ref 32, to the kinetic model used for NH_4ClO_4 . Even on this scale, the initial surface reaction is not visible while the exponential process ($33 \text{ min} < t < 60 \text{ min}$) can barely be distinguished.

obey (2.18) over a substantial range of a , this would indicate some type of branching.

3. Initial Reaction and Induction Period

An $a(t)$ plot for the thermal decomposition of NH_4ClO_4 on a large scale, $0 < a < 3 \times 10^{-4}$, shows²¹ the initial decomposition ($a_s = 3 \times 10^{-5}$) followed by a linear process which is succeeded by a rapid acceleration of the reaction at $a = 1.2 \times 10^{-4}$. Figure 1 of ref 22 shows nucleation along surface steps, plus a few isolated surface nuclei, on the \mathbf{m} or (210) face of the orthorhombic crystal heated to 205 °C for 15 min. In contrast, the \mathbf{c} , or (001), face of the same crystal is covered with small nuclei. Their average diameter is $3 \mu\text{m}$, and their density is $2 \times 10^6 \text{ cm}^{-2}$. Since the products are all gaseous, these initially-formed nuclei are just pancake-shaped holes. Assuming a depth of $\sim 1 \mu\text{m}$, the fractional decomposition calculated is 3×10^{-5} . After 25 min at 205 °C, these nuclei are unchanged, showing that nucleation occurs very rapidly at special sites but then growth stops when they reach a critical size. The decomposition from these nuclei can therefore be identified, with a_s . Nucleation sites are undoubtedly the points of emergence of dislocations, for in strained crystals, the nuclei on the \mathbf{c} face are aligned along [010],²² which is also one of the directions of etch-pit alignments both in NH_4ClO_4 ^{26,27} and in isomorphous BaSO_4 .²⁸ Why does reaction cease so dramatically? This could be because reaction occurs initially in strained crystal and these nuclei cease growing once the strained region is removed. Alternatively, special chemical conditions exist in NH_4ClO_4 because the primary step consists of proton transfer to give NH_3 and HClO_4 , which then undergo secondary chemical reactions.^{29,30} HClO_4 has a positive catalytic effect on the decomposition, while NH_3 has a negative catalytic effect.³¹ Possibly, water retained during slow crystallization from aqueous solution plays a role, the circular shape of the pits being due to chemical reaction in a temporary solution phase and the lack of further growth of these surface nuclei to the loss of water by evaporation.²³ The nuclei on the \mathbf{m} face are also of a remarkably uniform size. This suggests that the linear process is due to the slow inward growth of the surface nuclei.³² This is succeeded by a short exponential process^{21,32} usually attributed to branching nuclei. In NH_4ClO_4 , this can be associated with chains of nuclei spreading along favored crystallographic directions.²² The main part of the reaction obeys the Avrami equation (eq 2.12), due to continued formation and growth of nuclei in the bulk of the reactant. Figure 3 shows the fit of this model for $a \leq 3 \times 10^{-3}$, though even on this scale the exponential process ($33 \text{ min} < t < 60 \text{ min}$) is hardly visible.

4. Slow Growth

Although phenomenologically it may be impossible to distinguish a separate induction period from a period of slow

nucleus growth (in some cases the observed induction period is due to slow growth), it is convenient to do so from an interpretative or kinetic viewpoint. It is easy to believe that the kinetic conditions (for example, the activation energy) at a very small nucleus containing a few atoms are very different from those of nuclei of observable size. We have no knowledge of how the first few hundred atoms are added to a nucleus, but once a geometric shape is established, a circle, a cylinder, a hemisphere, or something more complicated⁴ when growth rates are different in different directions, one can make conjectures about the rate of decomposition at established but still submicroscopic nuclei. The product reactant interface is a strained one, and one can readily suppose therefore that the rate of decomposition depends on the size of the nucleus in some way. The simplest assumptions are that the rate depends on (a) the diameter of a nucleus, (b) the perimeter of a circular nucleus, (c) the area of a circular nucleus or volume of a hemispherical nucleus, or (d) the surface area of a hemispherical nucleus. However, the kinetic law and the rate constant are as yet undefined. We now make the hypotheses that the same rate law, $F(a) = kt$, that holds for large nuclei holds also for submicroscopic nuclei, but with a "rate constant" k that (in the range $a_0 < a < a^*$) depends on the amount decomposed. The special cases above then correspond to

- (a) $k(a) = k_s a^{1/3}$
- (b) $k(a) = k_s a^{1/2}$
- (c) $k(a) = k_s a$
- (d) $k(a) = k_s a^{2/3}$

So, in general, this model for slow growth supposes that k should be replaced by $k_s a^m$, giving

$$[dF(a)/da] da/dt = k(a) = k_s a^m \quad a_0 < a < a^* \quad (4.1)$$

In the early stages of decomposition, the rate equation usually reduces to a power law,

$$F(a) = [-\ln(1 - a)]^{1/n} \approx a^{1/n} = kt \quad (4.2)$$

$$(1/n)a^{(1/n)-1} da/dt = k_s a^m \quad (4.3)$$

If $mn \neq 1$, then

$$(1 - mn)^{-1} [a^{(1/n)-m} - a_0^{(1/n)-m}] = k_s(t - t_0) \quad a_0 < a < a^* \quad (4.4)$$

$mn = 1$ is a special case, for which

$$a = a_0 \exp[k_s n(t - t_0)] \quad a_0 < a < a^* \quad (4.5)$$

Thus, an exponential increase of a with t over a limited range of a may be due to slow growth with particular values of m and n . To examine the response of the Avrami equation (eq 2.12) to a variable k , and specifically the slow-growth model formulated above, consider the case in which, for $a < a^*$, the growth rate constant varies linearly with the volume of a hemispherical nucleus so that $k = k_s a$ and $m = 1$. Since $n = 4$,

$$a^{-3/4} - a_0^{-3/4} = -3k_s(t - t_0) \quad a_0 < a < a^* \quad (4.6)$$

According to the model, a constant growth rate is achieved at

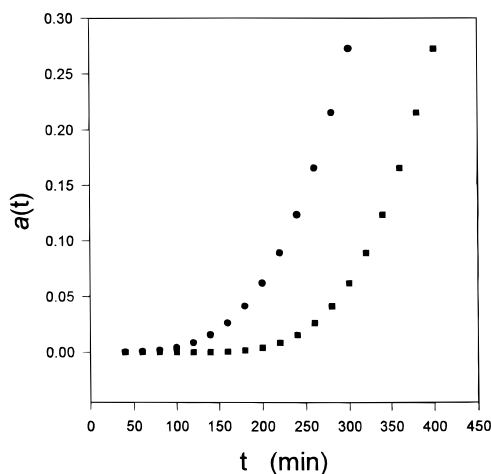


Figure 4. Plots of $a(t)$ for data that fit the Avrami equation (●) and data calculated from (4.6) for $a_0 < a < a^*$ (■). The figure demonstrates that the effect of slow growth is to shift the $a(t)$ curve along the time axis, that is, to introduce an induction period.

$a = a^*$ and eq 2.12 holds for $a > a^*$. The effect of kinetics controlled by (4.6) for $a_0 < a < a^*$ is shown in Figure 4, in comparison with “normal” Avrami kinetics calculated from (2.12). The latter are the same data as those plotted in Figure 1 but on an expanded scale to show the effect of slow growth. The second curve shows that the effect of slow growth is to displace the $a(t)$ curve along the time axis, that is, to introduce an induction period. The same effect can be illustrated by plotting $a^{1/n}$ (here $n = 4$) against t , when the linear curve is displaced along the time axis, which is equivalent to replacing t by $t - t_0$. The model does presume some initial decomposition a_0 , and in the calculations for Figure 4, a_0 was taken arbitrarily as 10^{-7} . Any reasonable value would do equally well.

A clear example of the slower initial rate of growth of nuclei is provided by the measurements of Cooper and Garner⁶ of dehydration nuclei on crystals of chrome alum. The nuclei present a circular shape to an observer and are three-dimensional and so are taken to be hemispherical, of volume σx^3 where x is the diameter of a nucleus and $\sigma = \pi/12$. Using $da/dt = k_s a^m$,

$$dx/dt = k\sigma' x^{3m} \quad (4.7)$$

with $\sigma' = \sigma^{(3m+2)/3}$. The experimental data before d/dt becomes constant confirm that

$$(dx/dt)^{1/3} = Sx + c \quad (4.8)$$

so that $m = 1$. c/S could be interpreted as some initial size of the nucleus before it starts growing, but we may not determine this size since the time axis has an arbitrary origin in the experimental data. From (7)

$$(x_0 + c)^{-2} - (x + c)^{-2} = 2S^3(t - t_0) \quad (4.9)$$

Experimental values of the diameter x of one of the nuclei from Figure 2 of ref 6 are shown in Figure 5, along with values of x calculated from (4.9), using values of S and c found from the experimental data using (4.8). Figure 5 shows that the model for slow growth of small nuclei provides a satisfactory quantitative explanation of the initial nonlinear increase in x with time. For larger values of x , the plots of $x(t)$ are accurately linear.⁶ The validity of the form of (4.9) implies that of (4.7) and, hence, the validity of the slow growth hypothesis $k = k_s a^m$.

As a second example, we consider the thermal decomposition of freshly-prepared mercury fulminate.³³ This reaction shows a long induction period (e.g., Figure 3 of ref 33), which is a

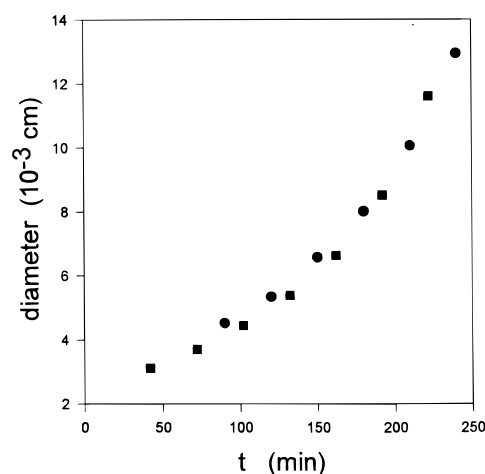


Figure 5. Diameter of a growing nucleus during the dehydration of chrome alum. Circles, experiment;⁶ squares, calculated from the model for slow growth with $m = 1$. The last experimental point marks the onset of the linear increase in diameter x with time. The zero on the time axis is arbitrary because it is so in the experimental data.

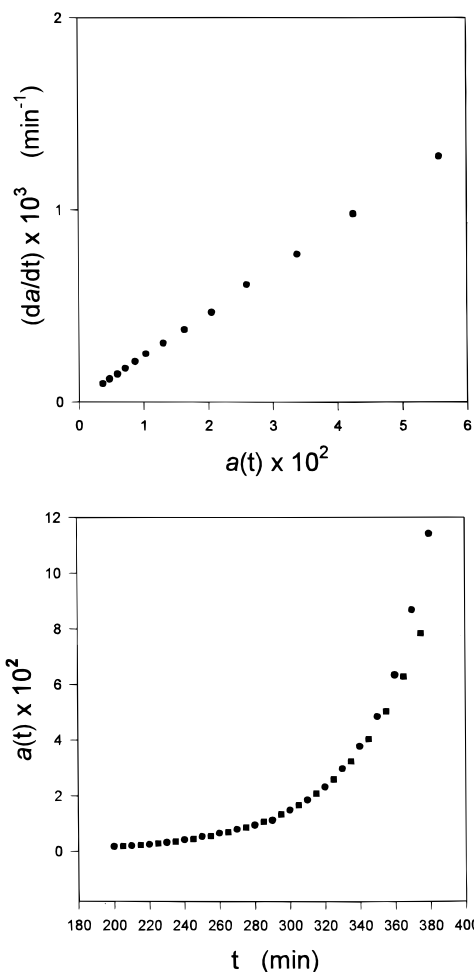


Figure 6. (a, top) Plot of da/dt against a for the thermal decomposition of mercury fulminate, using data from ref 33. (b, bottom) Experimental³³ (●) and calculated (■) values of $a(t)$ for the thermal decomposition of mercury fulminate.

good indication of slow growth. The plot of da/dt against a (Figure 6a) is accurately linear. After the slow-growth stage is over and a normal (constant) rate of growth ensues, a is proportional to t^3 so that $n = 3$ and

$$da/dt = k_s n a^{(2+3m)/3} \quad (4.10)$$

Since here $(2+3m)/3 = 1$, $m = 1/3$, which is case a above. Since here $mn = 1$, the model predicts that

$$\ln(a/a_0) = k_s n(t - t_0) \quad (4.11)$$

Calculated and experimental values of $a(t)$ are plotted against t in Figure 6b. The agreement is excellent up to the end of the slow-growth period at $t^* = 350$ min. For longer times, the decomposition data obey the cube law, $a^{1/3} = kt$, associated with the constant three-dimensional rate of growth of a fixed number of nuclei. This is why the experimental points lie above the curve calculated from (4.5) for $t > t^*$.

Experimental data for the thermal decomposition of nickel oxalate^{34,35} show the usual sigmoid curve for $a(t)$ with an initial surface reaction that accounts for about 1% of a , followed by a long induction period. The main part of the reaction, $0.05 < a < 0.90$, obeys the Erofe'ev equation with $n = 2$, indicating two-dimensional growth of rapidly-formed nuclei. The long induction period before the Erofe'ev equation holds, as well as the accelerating decomposition between $a_0 = 0.01$ and $a^* \approx 0.05$, is indicative of the slow growth of these nuclei. Since $n = 2$, $m = 1/2$ would lead to an exponential law which was found not to fit the data;³⁴ however, $m = 1$ would require that

$$a_0^{-1/2} - a^{-1/2} = k_s(t - t_0) \quad a_0 < a < a^* \quad (4.12)$$

which provides an excellent fit to the data. We may test the model by determining $k(a)$ directly from the gradient of $F(a) = kt$. Plots of $k(a)$, determined in this way, against a for the decomposition of the dihydrate at different temperatures verify the linear dependence of k on a during slow growth. Plots of $\log k_s$ vs T^{-1} obey the Arrhenius equation, and the activation energy from k_s for nickel oxalate dihydrate is $74\,400 \text{ kJ mol}^{-1}$, which is some $12\,700 \text{ kJ mol}^{-1}$ higher (as one would expect) than the activation energy from k for nuclei that are growing at a constant rate. The reasons for this difference at the atomistic level are not known, but it implies that the catalytic properties of nanoparticles of nickel are indeed different from those of a much larger size. Arrhenius behavior for k_s implies that the enthalpy of activation changes discontinuously at $a = a^*$, perhaps due to structural changes at the interface.

5. Branching Nuclei

An exponential dependence of a on t in the initial stages of the thermal decomposition of a solid may imply the slow growth of the first-formed nuclei with the special conditions $mn = 1$ (ref 4) or it may be due to branching nuclei (refs 2 and 3), a possibility that we shall now examine in greater detail.

An alternative to the grain-boundary model (which realistically can predict an exponential law over only a limited range of a) is one in which the growth of the first-formed nuclei generates the conditions for continued reaction due to the formation of dislocations, and even cracks, at the strained interface between product and reactant. Thus, each growing nucleus generates new nuclei, a process formally described as "branching". However, as reaction proceeds, the branching is curtailed (the usual description is that the branching chains are terminated) because the reaction is spreading into material that is already decomposed. In this model, which is due originally to Prout and Tompkins,³⁶ the rate of reaction is proportional to the amount decomposed, as in eq 2.17, but the rate constant now is the difference between the probability of branching k_b and that of termination $k_t a$. (The probability of termination depends on a because the greater a is, the greater the probability of a chain being terminated.) Therefore,

$$da/dt = (k_b - k_t a)a \quad (5.1)$$

At the point of inflection (a_i, t_i)

$$[d^2a/dt^2]_{a_i} = (k_b - 2k_t a_i) = 0 \quad k_t = k_b/2a_i \quad (5.2)$$

Assuming that the ratio k_t/k_b is independent of a ,

$$da/dt = k_b a(1 - a/2a_i) \quad a \geq a_0 \quad (5.3)$$

$$\ln \left[\frac{a}{1 - a/2a_i} \right] - \ln \left[\frac{a_0}{1 - a_0/2a_i} \right] = k_b(t - t_0) \quad (5.4)$$

where a_0 is the extent of the initial decomposition that takes place (during $0 < t \leq t_0$) prior to the chain-branching process dominating the kinetics of the reaction. In some thermal decompositions, a_i is close to $1/2$, and when this is so

$$\ln[a/(1 - a)] - \ln[a_0/(1 - a_0)] = k_b(t - t_0) \quad (5.5)$$

Equation 5.5 is named for Prout and Tompkins,²⁹ though it is usually quoted without explicit representation of the constant term. Unless $a_i = 1/2$, the more general form (eq 5.4), which we term the generalized Prout–Tompkins (GPT) equation, should be used. The above derivation of (5.5) clarifies that the Prout–Tompkins (PT) equation involves three assumptions: (i) The first assumption is the assumed linear dependence of the probability of termination $k_t a$ on a . Clearly this probability should depend on a , and the linear assumption is merely the simplest functional form. (ii) If (i) holds, then eq 5.2 shows that $k_t = k_b/2a_i$ at $a = a_i$, the point of inflection in $a(t)$. Equation 5.3 then follows only if the second assumption that the ratio k_t/k_b is independent of a holds. (iii) The PT equation (eq 5.5) then follows only from the third assumption that $a_i = 1/2$. This requires that the generally sigmoid $a(t)$ curve should be symmetrical about a_i, t_i , which is by no means always true. The thermal decomposition of KMnO_4 does satisfy this criterion, and the data are well-fitted by eq 5.5, for example, in Figures 2 and 3 of ref 36. For whole crystals of KMnO_4 , for example, the PT equation holds for $t_0 > 14$ min over the remarkable range $0.01 < a < 0.985$. $a_0 = 0.01$ seems an entirely reasonable value. The slope of the plot of $\ln[a/(1 - a)]$ against t is k_b , and the authors' analysis shows that different values of k_b hold during the acceleratory and decay periods, a point that needs further elucidation in terms of the PT model. It is not too surprising that k_b depends on a , but its constancy over the two regimes $a < a_i$ and $a > a_i$, with a discontinuous, or at least very sharp, change at a_i , has not been explained satisfactorily.

In contrast to KMnO_4 , the $a(t)$ curves for AgMnO_4 are not symmetrical about a_i . The generalized model has therefore been tested for the decomposition of the whole crystals of AgMnO_4 at 108°C . Figure 7 shows the plot of $F(a) = \log[a/(1 - a/2a_i)]$ against t using data from ref 37. Equation 5.4 provides a satisfactory fit to the data over the range $0.004 < a < 0.75$, compared to the original PT equation (eq 5.5) which fits the data only up to $a = 0.16$. Here $a_i = 0.466$, which seems not to be very different from 0.5 but nevertheless makes a big difference in the fitting of the data. The upper limit for (5.4) is $2a_i$ or 0.892 in this case. With original data available, a better procedure would be to fit $a(t)$ to (5.4) using a nonlinear least-squares program to determine a_0, t_0 , and k_b . However, Figure 7 is a sufficient illustration of the need to use (5.4) when a_i is not equal to 0.5. A more extreme case is provided by data for the decomposition of ground crystals of AgMnO_4 at 100°C .³⁷ The $a(t)$ curve is very unsymmetrical with $a_i = 0.213$. Figure 8 shows that the data are fitted by the GPT equation in the

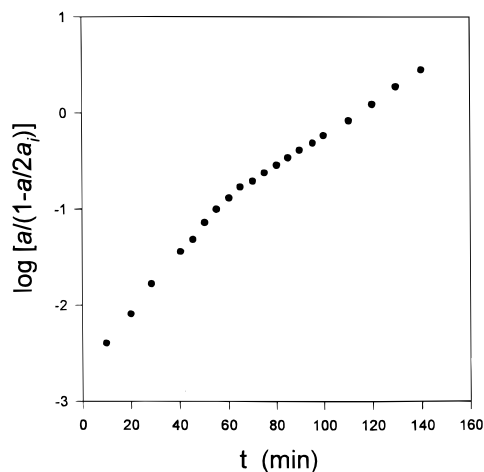


Figure 7. Test of (5.4) for the thermal decomposition of whole crystals of silver permanganate at 108 °C. Experimental data from ref 37.

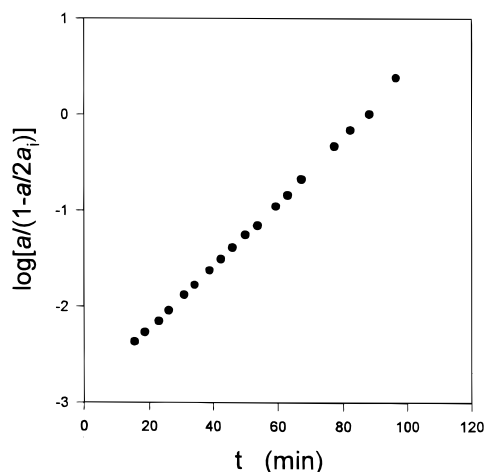


Figure 8. Tests of (5.4) for the thermal decomposition of ground crystals of silver permanganate at 100 °C. Experimental data from ref 37.

range $0.007 < a < 0.362$, compared to the PT equation which fits the data up to $a = 0.223$. $a = 0.362$ is the practical upper limit for the graphical representation of (5.4) because $2a_i = 0.426$. Because the upper limit of the data plotted is 0.362, a single value of k_b suffices.

6. Conclusions

The induction period has always been a rather baffling feature of the kinetics of the thermal decomposition of solids. The new analysis in this paper shows that this may be in association with the slow initial rate of growth of nuclei. The general phenomenological model formulated has been shown to provide a quantitative explanation of the early-stage kinetics in three widely different examples, the dehydration of chrome alum, the decomposition of the metal salt of an organic acid, nickel oxalate, and the slow decomposition of the explosive mercury

fulminate. This leads to the expectation that the model may prove to be of wider utility. The model of branching nuclei (due to structural changes in the reactant) has been reformulated, and the approximations that it involves have been emphasized. A new equation called the generalized Prout–Tompkins equation is shown to provide a much better fit to the data in cases where the $a(t)$ decomposition curve is not symmetrical at $a = 1/2$.

References and Notes

- (1) For a modern assessment, see Boldyrev, V. V., ed. *Reactivity of Solids: Past Present and Future*; Blackwell Science: Oxford, 1996.
- (2) Schmalzried, H. *Chemical kinetics of Solids*; VCH, Weinheim, 1995.
- (3) Allnatt, A. R.; Jacobs, P. W. M. *Can. J. Chem.* **1968**, *46*, 111.
- (4) Bright, N. F. H.; Garner, W. E. *J. Chem. Soc. London* **1934**, 1872.
- (5) Garner, W. E.; Southon, W. R. *J. Chem. Soc. London* **1935**, 1705.
- (6) Cooper, J. A.; Garner, W. E. *Trans. Faraday Soc.* **1936**, *32*, 1739.
- (7) Wishcin, A. *Proc. R. Soc. London A* **1939**, *172*, 314.
- (8) Acock, G. P.; Garner, W. E.; Milsted, J.; Willavoy, H. J. *Proc. R. Soc. London A* **1947**, *189*, 508.
- (9) Bagdassarian, Kh. S. *Acta Physicochem. URSS* **1945**, *20*, 441.
- (10) Jacobs, P. W. M. *Kinetics of Reactions in Ionic Systems. Materials Science Research*; Plenum: New York, 1969; Vol. 4, p 37.
- (11) Tompkins, F. C. In *Treatise on Solid State Chemistry*; Hannay, N. B., Ed.; Plenum: New York, 1976; Vol. 4, p 193.
- (12) Mościński, J.; Jacobs, P. W. M. *Proc. R. Soc. London A* **1985**, *398*, 141.
- (13) Galwey, A. K. *React. Solids* **1990**, *89*, 211.
- (14) Jacobs, P. W. M.; Tompkins, F. C. In *Chemistry of the Solid State*, Garner, W. E., Ed.; Butterworths: London, 1955; Chapter 7.
- (15) Young, D. A. *Decomposition of Solids*; Pergamon: Oxford, 1966.
- (16) Mampel, K. L. *Z. Phys. Chem. A* **1940**, *187*, 43, 235.
- (17) Bradley, R. S.; Colvin, J.; Hume, J. *Proc. R. Soc. London A* **1932**, *137*, 531.
- (18) Erofe'ev, B. V. *Compt. Rend. Acad. Sci. URSS* **1946**, *52*, 511.
- (19) Avrami, M. *J. Chem. Phys.* **1939**, *7*, 1103; **1940**, *8*, 212; **1941**, *9*, 177.
- (20) Johnson, W. A.; Mehl, R. F. *Trans. AIME* **1939**, *135*, 416.
- (21) Jacobs, P. W. M.; Ng, Wee Lam. *7th Int. Symp. on Reactivity of Solids*; Chapman & Hall: London, 1972; p 398.
- (22) Herley, P. J.; Jacobs, P. W. M.; Levy, P. W. *Proc. R. Soc. London A* **1970**, *318*, 197.
- (23) Galwey, A. K.; Herley, P. J.; Mohamed, M. A. *React. Solids* **1988**, *6*, 205.
- (24) Garner, W. E.; Hailes, H. R. *Proc. R. Soc. London A* **1933**, *139*, 576.
- (25) Finch, A.; Jacobs, P. W. M.; Tompkins, F. C. *J. Chem. Soc. London* **1954**, 2053.
- (26) Williams, J. O.; Thomas, J. M.; Savintsev, Y. P.; Boldyrev, V. V. *J. Chem. Soc. London A* **1971**, 1759.
- (27) Herley, P. J.; Jacobs, P. W. M.; Levy, P. W. *J. Chem. Soc. London A* **1971**, 434.
- (28) Williams, J. O.; Tennakoon, D. T. B.; Thomas, J. M.; Jacobs, P. W. M. *J. Chem. Soc., Faraday Trans.* **1972**, *68*, 1987.
- (29) Galwey, A. K.; Mohamed, M. A. *Proc. R. Soc. London A* **1984**, *396*, 425.
- (30) Jacobs, P. W. M.; Pearson, G. S. *Combust. Flame* **1969**, *13*, 419.
- (31) Davies, J. V.; Jacobs, P. W. M.; Russell-Jones, A. *Trans. Faraday Soc.* **1967**, *63*, 1737.
- (32) Jacobs, P. W. M.; Ng, Wee Lam. *J. Solid State Chem* **1974**, *9*, 315.
- (33) Bartlett, B. E.; Tompkins, F. C.; Young, D. A. *J. Chem. Soc. London* **1956**, 3323.
- (34) Jacobs, P. W. M.; Kureishy, A. R. T. *4th Symp. on Reactivity of Solids*; Elsevier: Amsterdam, 1960; p 361.
- (35) Jacobs, P. W. M.; Kureishy, A. R. T. *Trans. Faraday Soc.* **1962**, *58*.
- (36) Prout, E. G.; Tompkins, F. C. *Trans. Faraday Soc.* **1944**, *40*, 488.
- (37) Prout, E. G.; Tompkins, F. C. *Trans. Faraday Soc.* **1946**, *44*, 468.